Journal of Engineering Science and Technology
Vol. 21, No. 2 (2026) 313 - 325

IMPACT OF WATER SPRAYING TECHNIQUE ON HEAT REJECTED FROM SOLAR PANEL

SOUD ALI SOUD[1,2,*], DAYANG RADIAH AWANG BIAK[1], MOHAMAD REZI ABDUL HAMID[1], SHAFREEZA SOBRI[1]

[1]Department of Chemical & Environmental Engineering, Faculty of Engineering, Universiti Putra Malaysia, Selangor, 43400, Malaysia
[2]Department of Chemical Engineering, Al-Muthanna University, Samawah, 66001, Iraq
*Corresponding Author: soudali2010@mu.edu.iq

Abstract

A small amount of solar energy that is converted to power electricity. It is possible for residual energy to heat a solar cell, raising the panel's temperature. It results in an increase in the solar panel's heat rejection (losses) and causes the urban heat island (UHI) phenomena; therefore, making heat losses at the lowest level of heat rejection to the environment is crucial. A number of techniques have been employed to reduce the temperature of solar panel. The water spraying technique is one of active method to cold surface of module. In this investigation three factors were studied, including number of nozzles, space between nozzles and surface of module and volumetric flow rate of water. Response Surface Methodology RSM together with rotatable central composite design and full factorial method were utilised to create the work's experimental design, derive the mathematical model, and determine the ideal circumstances for the work that includes nozzles number of 4.52, nozzles to module distance of 16.53 mm and 3.19 L/min of volumetric flow rate of water.

Keywords: Heat losses, Photovoltaic module, Response surface methodology, Water spraying.

1. Introduction

The globe is moving towards renewable energy sources as a result of the depletion of natural resources like gas and crude oil [1, 2]. Renewable energy sources such as hydropower, biomass, solar, and wind are becoming more and more important on a global scale [3-5]. As compared to other sources of renewable energy solar energy has a large following due to its advantages of being clean, abundant, affordable, and simple to use. Based on its characteristics, solar energy has been widely used to meet human energy needs.

The commercially available photovoltaic technology usually has an energy conversion rate of five to twenty percent. Unfortunately, this rate is lowered due to the PV panel's continuous high-temperature operation. Efficiency typically decreases by 0.25-0.5% each degree Celsius [6, 7].

A lot of research has been done to find out how various environmental factors impact the efficiency of solar panels [8]. In addition, because of the properties of the crystalline silicone used in solar panels, the operating temperature of the solar cells can have a substantial impact on the electrical competence of photovoltaic modules. When temperatures rise, the amount of energy these cells produce drops [9, 10]. Reducing the surface temperature of solar cells can improve the efficiency of PV power generation[11].

Heat can travel in the PV panels by conduction, convection, and radiation. The exchange of heat energy between layers of PV panel is known as conduction. As a liquid or gas travels around PV panel, convection takes place. All bodies continuously release some thermal energy, and this energy can move between the PV panel and the environment via radiation.

There are many techniques to cool PV modules like; employing a green roof under solar panels [12], using phase change materials (PCM) [13], cooling by heat pipe [14], cooling via Forced air [15], evaporative cooling by using sprinklers [16], and forced watering of the PV panel's front surface [17].

The water spraying technique is one of the active methods to cool the surface of the module. It is very efficient, simple process and does not need to change the structure of solar panel [18]. Running water over the surface of a PV panel can also assist lowering losses by removing dust, dead leaves, and bird droppings [9,19].

Some studies related with water cooling like, study of Osma-Pinto and Ordonez-Plata [20] formed a novel dynamic thermal model (RC model) to calculate the temperature of photovoltaic cells (PV) during sporadic irrigation using two methods: one for when the front surface is not being irrigated and another for when the surface is being irrigated. Furthermore, da Silva et al. [21] developed and validated mathematical models, in addition to empirical assessments, for a water-film cooling system for commercial solar modules. Also, Shahverdian et al. [22] conducted a process of optimisation for a solar module's water cooling.

2. Experimental Setup

The trials were conducted out at engineering faculty of the Universiti Putra Malaysia (UPM). Figure 1 shows the research framework of this work.

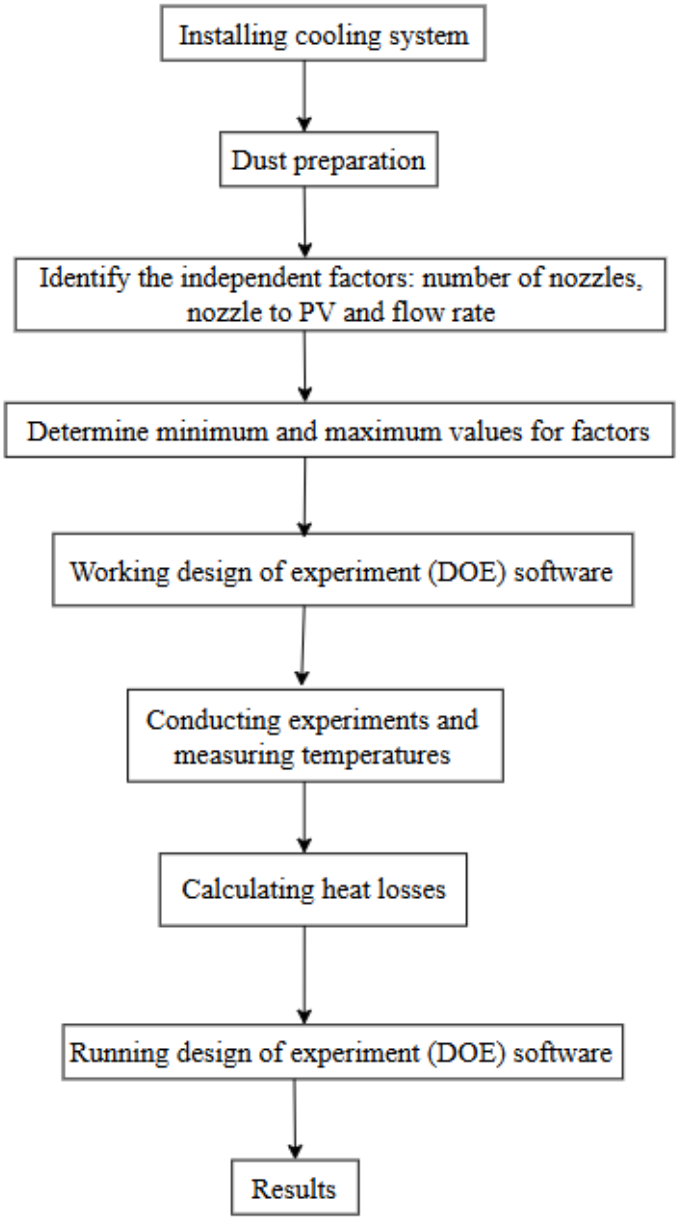

Fig. 1. The research framework.

2.1. Apparatus

The primary components of the cooling system are as follows: Two water tanks (collapsible rain barrel) of 100 L capacity, material PVC. Water pump (QB 60) of suction 8-9 meters, head max 15 meters, supply 27 litres/minute, rotating speed 2850 rpm, wattage 370 w and voltage 220 v-230 v. Liquid flow metre 0.2-2 GPM/1-7 LPM. Five water-nozzles with diameter 4 mm for spraying water on the PV panels. A water collection drainpipe.

A monocrystalline solar module with 36 solar cells. The technical specs for the module are displayed in Table 1. A monocrystalline solar module facing south with tilted 10 degrees [23]. System rig of experimental was displayed in Fig. 2.

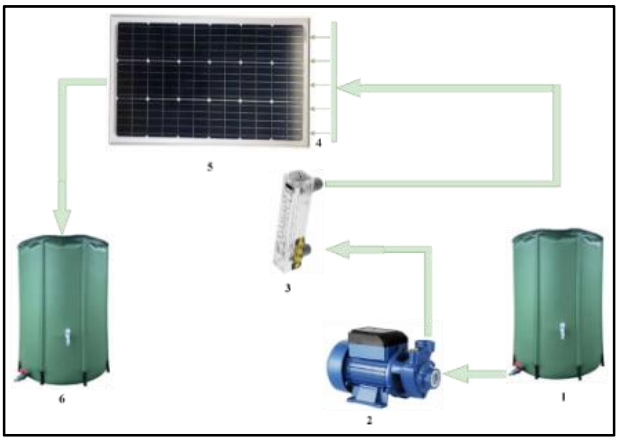

Fig. 2. Experimental rig system (1) Water tank, (2) Water pump, (3) Water flow meter, (4) Water nozzles, (5) Solar panel, (6) Water tank.

Table 1. The technical characteristics for the photovoltaic module.

Maxson Solar Panel	Model FNEF105-100
Maximum Power (*Pmax*)	100 W
Voltage at Pmax	18 V
Current at Pmax (Imp)	5.56 A
Open - Circuit Voltage (*Voc*)	21.6 V
Short - Circuit Current (*Isc*)	6.12 A
Power Tolerance	±3 W
Weight	7 kg
Dimensions	1025×542×30 mm

2.2. Dust preparation

A sample of dust from the University of Putra Malaysia soil was collected. The concrete fragments and other large solids were manually removed. According to Sarver et al. [24], the size of a sand particle is about 0.4 mm, so use a sieve with a 0.6 mm opening to get particles of this size. Then, the sample was put in a furnace (Memmert UFB 400) at 105°C for 24 hours to get a dry and humidity-free sample. The sample was then put through milling to create a homogeneous sample. This was accomplished using a Smooth Double Roll Crusher from Premur Group. After that, the sample was heated again to 105°C for 24 hours to remove any moisture.

The pace at which dust accumulates varies depending on the site environment. Dust densities with different places, period and season were show in Table 2 [25]. For this reason, in this study, worked with 8 g/m² of dust for each run. The weighing of dust was achieved using a balance (AND GF-300) with a maximum capacity of 310 g and high precision reaching 0.0001. Every experiment in this study uses sieve with a 0.6 mm opening to spread the dust evenly. The solar panel was cleaned of dust at the end of each test run. The dust was then collected and disposed of.

Table 2. Dust densities with different places, period and season.

Country	Dust density g/m²	Period and season	Reference
Saudi Arabia	5	45 days	Ilse et al. [26] and Said and Said and Walwil [27]
Pakistan	5.5	30 days	Ilse et al. [26]
Indonesia	3.8 1.7	Dry rainy	Tanesab et al. [28]
Algeria	8	Dry	Fathi et al. [29]
Iran	7.5	70 days	Gholami et al. [30]

3. Experimental design

A rotatable central composite design (CCD) with a full factorial method was utilized to plan the study's trials and create a mathematical model. This model describes the association between heat losses (response) together with the studied factors: number of nozzles, nozzle to PV and flow rate. Minitab 2019 was used as a tool.

Set of 20 experiments were conducted with base block one, six cube centre points, 6 axial points, 8 cube points. In which α = 1.68179 and level of significance = 0.05. The independent factors (predictors) employed in this study contained: number of nozzles (A), nozzles to PV distance (B) and water flow rate (C), while the dependent factor (response) was the heat losses. Table 3 displays amount of the autonomous factors at minimum and maximum values.

Table 3. Minimum and maximum values of input factors.

Coded factor	Factor name	Unit	Minimum value	Maximum value
A	number of nozzles	--	1	5
B	nozzles to PV	mm	10	50
C	flow rate	L/min	2	3.5

The software (DOE) was used, and Table 4 was obtained. The cooling system works for 50 seconds when the temperature exceeds 50 °C [31]. After that, the heat losses were calculated. It is the sum of the heat radiation loss, heat evaporation loss and heat convection loss. Heat losses were calculated using Eqs. (1)- (4) [32]. Radiation loss (Q_R) represents the heat exchanged between the glass layer of the PV panel and the environment. Evaporation loss ($Q_{evap.}$) represents the heat which water needs to evaporate. Convection loss (Q_C) represents the heat which water takes from the surface of the PV panel, and can be computed in the manner described below:

$$Q_R = \varepsilon \sigma \left(T_s^4 - T_{sky}^4 \right) \quad (1)$$

$$T_{sky} = 0.0552 \; T_a^{1.5} \quad (2)$$

$$Q_{evap.} = \dot{m} \lambda \quad (3)$$

$$Q_C = \dot{m} C_p \left(T_2 - T_1 \right) \quad (4)$$

Table 4. The central composite design and heat losses values for the experiment.

Std	Run	A	B	C	Response
		Number of nozzles	Nozzles to PV	Flow rate	Heat losses
		-	mm	L/min	kw/m²
6	1	4.189	18.107	3.195	7.035
3	2	1.810	41.892	2.304	6.413
2	3	4.189	18.107	2.304	6.355
18	4	3.000	30.000	2.750	10.487
8	5	4.189	41.892	3.195	5.770
13	6	3.000	30.000	2.000	6.083
20	7	3.000	30.000	2.750	10.407
19	8	3.000	30.000	2.750	9.741
14	9	3.000	30.000	3.500	7.358
15	10	3.000	30.000	2.750	11.702
1	11	1.810	18.107	2.304	5.252
5	12	1.810	18.107	3.195	7.178
16	13	3.000	30.000	2.750	10.044
12	14	3.000	50.000	2.750	5.930
4	15	4.189	41.892	2.304	7.200
7	16	1.810	41.892	3.195	10.139
17	17	3.000	30.000	2.750	11.695
10	18	5.000	30.000	2.750	7.699
11	19	3.000	10.000	2.750	4.650
9	20	1.000	30.000	2.750	7.252

4. Results and discussion

4.1. Mathematical model

The values of heat losses were recorded in Table 4. Through experimentation and analysis using CCD technique, the quadratic model that predicts the connection between the heat losses and the independent variables utilised in this study was created using the values listed in Table 4.

The outcomes indicate that the generated quadratic model is well-matched with the empirical data, with R^2 value 91.50 %, adjusted R^2 value 83.86 %, and a lack-of-fit p-value of 0.412. Equation (5) represents this model.

$$heat\ losses = -75.2 + 9.44\,A + 0.924\,B + 40.67\,C - 0.700\,A^2 - 0.01246\,B^2 - 6.32\,C^2 - 0.0401\,AB - 1.509\,AC - 0.0073\,BC. \quad (5)$$

This model has quadratic terms A, B, and C and interaction terms AB, AC, and BC.

Plotting predicted versus observed removal percentage figure allows for additional confirmation of the model's correctness. The responses' residual plot values are displayed in Figs. 3-7.

The residual plot's normal probability is displayed in Fig. 4(a). In this figure, the points fall near the line. This suggests that the distribution of the data is normal and deviation from normality is small, therefore proving the projected model's accuracy.

The fit of the residual plot is disclosed in Fig. 4(b). The data shown in this figure is to be randomly distributed with no discernible pattern, suggesting that the variance is constant, and that validates the projected model's accuracy.

The residual vs. order plot is displayed in Fig. 4(d). It is possible to determine whether the variables are associated with one another from this plot. The data dispersion at random verifies that there is no correlation between the variables, indicating the accuracy of the projected model.

A Pareto chart can be used to show and compare the significance of each variable's standardised effect level on the heat losses (Fig. 5). It illustrates that the independent factors have a declining effect on the heat losses according to the order of number of nozzles, nozzles to PV distance and water flow rate. The links between the experimental variables and how they influence the response are shown in Fig. 6.

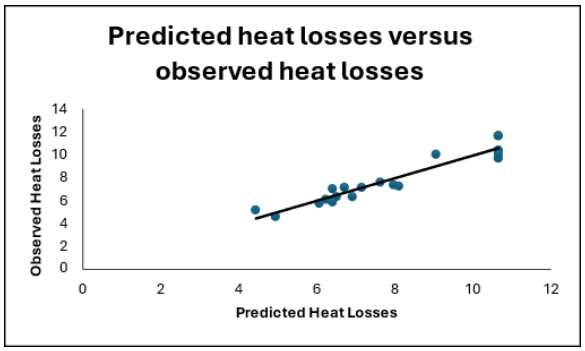

Fig. 3. Predicted vs. observed heat losses.

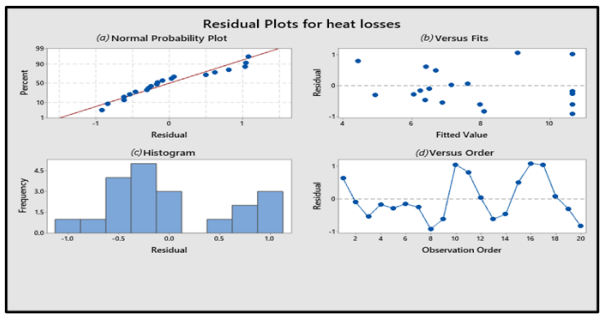

Fig. 4. Residual plots for heat losses (a) normal probability, (b) versus fits, (c) histogram and (d) observation order.

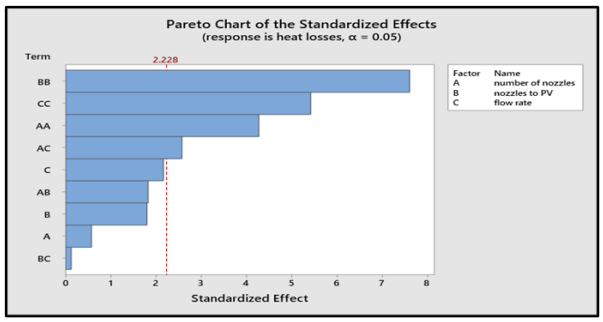

Fig. 5. Pareto chart of the standardised effects.

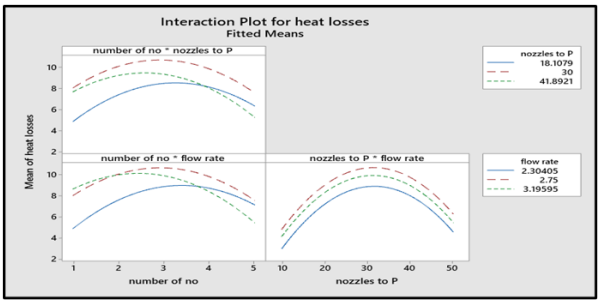

Fig. 6. Interaction plot for heat losses.

4.2. Effect of number of nozzles

As shown in Fig. 7(a), positive effects of the number of nozzles within the range of 1-3 on heat losses, due to increasing the spread area on the surface of module. At number above 3, the heat losses decreased because the spread area reduced due to decrease the velocity of water [33]. Increasing the number of nozzles will increase the flow area and this in turn reduces the flow velocity and hence reduce the heat losses.

4.3. Effect of nozzle to PV spacing

As shown in Fig. 7(b), positive effects of nozzle to PV spacing within the range of 10-30 mm on heat losses, due to water striking the surface of the PV module moderately, so few points are being cooled on the PV surface. At distance above 30 mm, the heat losses decreased because water hits strongly and the water splash on the plate is relatively greater, so more points are being cooled on the PV surface.

4.4. Effect of water flow rate

As shown in Fig. 7(c), positive effects of the volumetric flow rate within the range of 2-2.85 l/min on heat losses, due to increasing the spread area on the surface of module. At volumetric flow rate above 2.85 l/min, the heat losses decreased because the spread area reduced due to large volumetric flow rate. When the mass flow of water is large that the amount of radial dispersion of water becomes greater and the jet is spread at a greater distance in a radial direction reducing the heat losses [34].

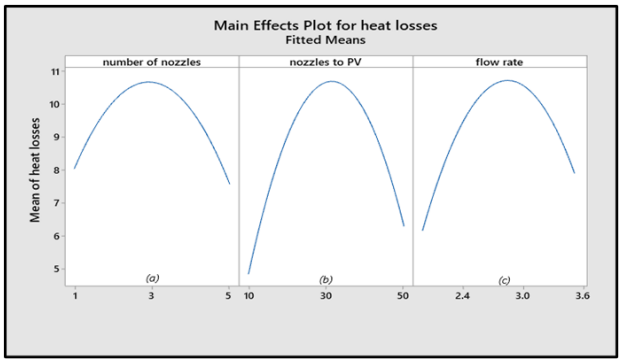

Fig. 7. Main effects plot for heat losses: (a) effect of number of nozzles, (b) effect of nozzles to PV spacing, and (c) effect of water flow rate.

5. Optimisation of process

The response surface methodology is a statistical design that works effectively for data analysis and mathematical model prediction, whereas the CCD is a useful tool for optimising independent factors and getting the best possible response.

The relationships between variables and their influences on heat losses are demonstrated through surface and contour plots of heat losses, as shown in Figs. 8 and 9.

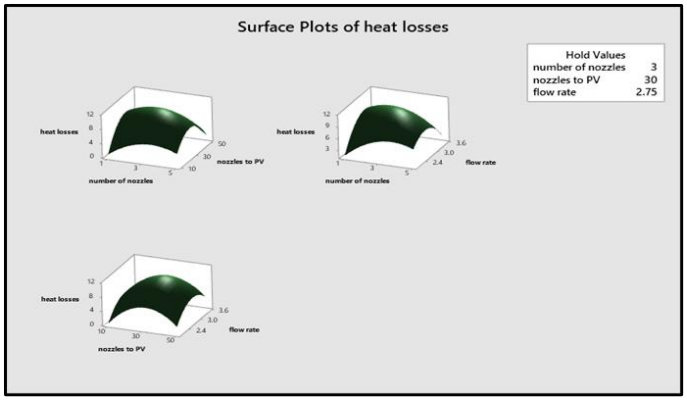

Fig. 8. Surface plot of heat losses vs utilised variables.

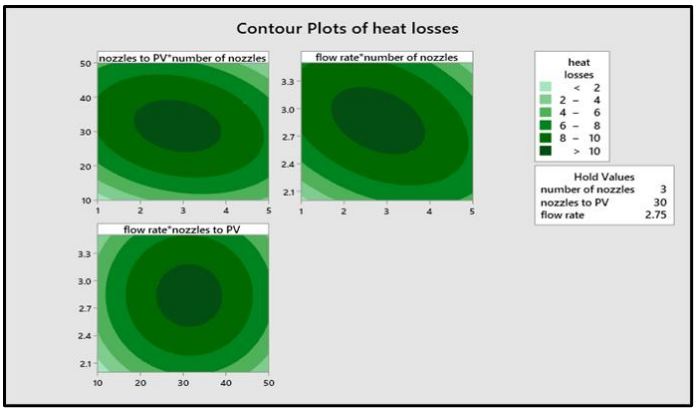

Fig. 9. Contour plot of heat losses vs utilised variables.

These figures were used to estimate the optimal conditions, and Table 5 's parameters were used to carry out the optimisation method. Table 6 displays the optimal circumstances necessary to get the optimal response (minimum heat losses of 5.25).

Table 5. Parameter settings for optimisation.

Response	Heat losses
Goal	Minimum
Target	5.25
Upper	11.702
Weight	1
Importance	1

Table 6. Optimum conditions.

Solution	1
Number of Nozzles	4.52
Nozzles to PV	16.53
Flow rate	3.19
Heat losses fit	5.25
Composite desirability	1

The optimum conditions, which included several nozzles of 4.52, nozzles to PV distance of 16.53 mm, and water flow rate of 3.19 L/min, were tested experimentally with 5, 16.55, and 3.20, respectively. The result showed that the heat losses was 5.5 kw/m². Whereas the predicted value is 5.25 kw/m². The difference between the observed and expected value is used to compute the percentage deviation using the relationship below [35]:

$$\text{percentage deviation} = \frac{\text{observed}-\text{expected}}{\text{observed}} \times 100 \quad (6)$$

The percentage deviation was 4.54%. This verified that the expected model was correct.

6. Conclusions

This study explores the effectiveness of a water spraying technique in reducing heat losses from photovoltaic (PV) panels across 20 experimental runs. Utilizing Design of Experiments (DOE) and Response Surface Methodology (RSM), a predictive model was developed to identify optimal operating conditions. The primary findings from the study are as follows:

- A mathematical model describing the relationship between heat losses and the selected factors was developed and validated using response surface methodology and a central composite design.
- The RSM model exhibited strong predictive accuracy ($R^2 > 0.9$), confirming its reliability for performance optimization.
- The optimal conditions for minimizing heat losses (5.25 kw/m²) were determined to be 4.52 nozzles, 16.53 mm nozzles-to-PV spacing, and a water flow rate of 3.19 L/min.

Based on the optimized results from the RSM model, the combination of nozzle count, nozzle-to-PV panel distance, and water flow rate was found to significantly reduce heat losses in photovoltaic systems. Furthermore, RSM proved to be a robust and reliable method for analysing the individual and interactive effects of these parameters on thermal performance.

7. Limitations

The limitation of this study was that environmental parameters like relative humidity was excluded. The sidewinds were not included.

8. Future Work

The next tips are recommendations that the current study can be expanded:

- The chemical and physical characteristics of dust must be examined, as well as how they affect heat transfer.
- The side winds and environmental factors like relative humidity must be considered, as well as how they affect heat transfer.
- Study the impact of heat rejection on the environment for other solar energy systems.

Nomenclature	
c_p	Specific heat (KJ/Kg °C)
Imp	Current at Pmax (A)
Isc	Short circuit current (A)
ṁ	Mass flow rate (kg/sec)
Pmax	Maximum power (W)
Q_C	Heat convection loss (W/m²)
$Q_{evap.}$	Heat evaporation loss (W/m²)
Q_R	Heat radiation loss (W/m²)
Ta	Ambient temperature (°C)
Ts	Surface temperature (°C)
Tsky	Sky temperature (°C)
T_1	Water tank temperature (feed) (°C)
T_2	Water tank temperature (drain) (°C)
Voc	Open circuit voltage (V)
Greek symbols	
ε	Emissivity of the glass
λ	Latent heat of evaporation (kJ/kg)
σ	Stefan Boltzmann constant (5.68×10^{-8} W/m² K⁴)
Abbreviations	
CCD	Central composite design
DOE	Design of experiment
GPM	Gallon per minute
LPM	Liter per minute
PCM	Phase change materials
PV	Photovoltaic module
PVC	Polyvinyl chloride
UHI	Urban heat islands
UPM	Universiti Putra Malaysia

References

1. Gielen, D. et al. (2019). The role of renewable energy in the global energy transformation. *Energy Strategy Reviews,* 24, 38-50.
2. Khalid, H.M. et al. (2023). Dust accumulation and aggregation on PV panels: an integrated survey on impacts, mathematical models, cleaning mechanisms, and possible sustainable solution. *Solar Energy*, 251, 261-285.
3. Vinod; Kumar, R.; and Singh, S.K. (2018). Solar photovoltaic modeling and simulation: as a renewable energy solution. *Energy Reports*, 4, 701-712.
4. Xu, L. et al. (2020). The influence of dust deposition on the temperature of soiling photovoltaic glass under lighting and windy conditions. *Solar Energy*, 199, 491-496.

5. Soroush, M.; and Hajimolana, Y. (2023). Sunlight harvesting. *Computers and Chemical Engineering*, 170, 108103.
6. Koohestani, S.S.; Nižetić, S.; and Santamouris, M. (2023). Comparative review and evaluation of state-of-the-art photovoltaic cooling technologies. *Journal of Cleaner Production*, 406, 136953.
7. Hassan, R.; and Aboaltabooq, M.H.K. (2021). Photovoltaic panel cooling: a review of methodologies and technologies. *Al-Furat Journal of Innovations in Mechanical and Sustainable Energy Engineering*, 1(1), 55-56.
8. Rabaia, M.K.H. et al. (2021). Environmental impacts of solar energy systems: A review. *Science of the Total Environment*, 754, 141989.
9. Azimi, A.; Basiri, N.; and Eslami, M. (2024). A novel two-step optimization approach for film water cooling of a photovoltaic module in real ambient conditions. *Applied Thermal Engineering*, 236, 121898.
10. Hasan, I.A.; Mohammed, M.J.; and Attallah, M. (2022). Analytical and experimental performance evaluation of direct flow cooling effect on PV panel. *Proceedings of the* 2*nd international conference on electromechanical engineering and its applications* [*icemea2021*], Baghdad, Iraq, 020013.
11. Li, J.; Xi, Z.; and Wu, S. (2019). Performance of autonomous temperature controlled photovoltaic modules with water film. *IOP Conference Series*: *Earth and Environmental Science*, 267(3), 032097.
12. Osma-Pinto, G.; and Ordóñez-Plata, G. (2019). Measuring factors influencing performance of rooftop PV panels in warm tropical climates. *Solar Energy*, 185, 112-123.
13. Agarwal, N.; and Saxena, A. (2022). Performance characteristics of a photovoltaic panel integrated with PCM packed cylindrical tubes for cooling. *International Journal of Sustainable Energy*, 41(5), 444-468.
14. Alizadeh, H. et al. (2018). Numerical simulation of PV cooling by using single turn pulsating heat pipe. *International Journal of Heat and Mass Transfer*, 127, 203-208.
15. Sajjad, U.; Amer, M.; Ali, H.M.; Dahiya, A.; and Abbas, N. (2019). Cost effective cooling of photovoltaic modules to improve efficiency. *Case Studies in Thermal Engineering*, 14, 100420.
16. Zilli, B.M. et al. (2018). Performance and effect of water-cooling on a microgeneration system of photovoltaic solar energy in Paraná Brazil. *Journal of Cleaner Production*, 192, 477-485.
17. Osma-Pinto, G.; and Ordóñez-Plata, G. (2019). Measuring the effect of forced irrigation on the front surface of PV panels for warm tropical conditions. *Energy Reports*, 5, 501-514.
18. Dwivedi, P.; Sudhakar, K.; Soni, A.; Solomin, E.; and Kirpichnikova, I. (2020). Advanced cooling techniques of P.V. modules: A state of art. *Case Studies in Thermal Engineering*, 21, 100674.
19. Amran, N.M.H.N. et al. (2023). Effect of water cooling and dust removal on solar photovoltaic module efficiency. *Journal of Advanced Research in Fluid Mechanics and Thermal Sciences*, 105(1), 184-193.
20. Osma-Pinto, G.; and Ordóñez-Plata, G. (2020). Dynamic thermal modelling for the prediction of the operating temperature of a PV panel with an integrated cooling system. *Renewable Energy*, 152, 1041-1054.

21. da Silva, V.O. et al. (2021). Theoretical and experimental research to development of water-film cooling system for commercial photovoltaic modules. *IET Renewable Power Generation*, 15(1), 206-224.
22. Shahverdian, M.H. et al. (2021). A dynamic multi-objective optimization procedure for water cooling of a photovoltaic module. *Sustainable Energy Technologies and Assessments*, 45, 101111.
23. Jacobson, M.Z.; and Jadhav, V. (2018). World estimates of PV optimal tilt angles and ratios of sunlight incident upon tilted and tracked PV panels relative to horizontal panels. *Solar Energy*, 169, 55-66.
24. Sarver, T.; Al-Qaraghuli, A.; and Kazmerski, L.L. (2013). A comprehensive review of the impact of dust on the use of solar energy: History, investigations, results, literature, and mitigation approaches. *Renewable and Sustainable Energy Reviews*, 22, 698-733.
25. Sakarapunthip, N.; Chenvidhya, D.; Chuangchote, S.; and Chenvidhya, T. (2021). Dust accumulation and its effect on PV performance in tropical climate and rice farm environment. *Proceedings of the IEEE* 48*th Photovoltaic Specialists Conference* (*PVSC*), Fort Lauderdale, USA, 1848-1854.
26. Ilse, K.K. et al. (2018). Comprehensive analysis of soiling and cementation processes on PV modules in Qatar. *Solar Energy Materials and Solar Cells*, 186, 309-323.
27. Said, S.A.M.; and Walwil, H.M. (2014). Fundamental studies on dust fouling effects on PV module performance. *Solar Energy*, 107, 328-337.
28. Tanesab, J.; Parlevliet, D.; Whale, J.; and Urmee, T. (2017). Seasonal effect of dust on the degradation of PV modules performance deployed in different climate areas. *Renewable Energy*, 111, 105-115.
29. Fathi, M.; Abderrezek, M.; and Grana, P. (2017). Technical and economic assessment of cleaning protocol for photovoltaic power plants: Case of Algerian Sahara sites. *Solar Energy*, 147, 358-367.
30. Gholami, A.; Saboonchi, A.; and Alemrajabi, A.A. (2017). Experimental study of factors affecting dust accumulation and their effects on the transmission coefficient of glass for solar applications. *Renewable Energy*, 112, 466-473.
31. Yesildal, F.; Ozakin, A.N.; and Yakut, K. (2022). Optimization of operational parameters for a photovoltaic panel cooled by spray cooling. *Engineering Science and Technology, an International Journal*, 25, 100983.
32. Holman, J.P. (2010). *Heat transfer*. McGraw-Hill series in mechanical engineering.
33. Elnozahy, A.; Rahman, A.K.A.; Ali, A.H.H.; Abdel-Salam, M.; and Ookawara, S. (2015). Performance of a PV module integrated with standalone building in hot arid areas as enhanced by surface cooling and cleaning. *Energy and Buildings*, 88, 100-109.
34. Javidan, M.; and Moghadam, A.J. (2021). Experimental investigation on thermal management of a photovoltaic module using water-jet impingement cooling. *Energy Conversion and Management*, 228, 113686.
35. Das, S.; Biswas, A.; and Das, B. (2023). Parametric investigation on the thermo-hydraulic performance of a novel solar air heater design with conical protruded nozzle jet impingement. *Applied Thermal Engineering*, 219, 119583.